A-source Inverter-fed PMSM drive with fault-tolerant capability for Electric Vehicles

Vivek Sharma[1*], Subhas Mukhopadhyay[2], M. J. Hossain[3], S. M. Nawazish Ali[4], and Muhammad Kashif[5]

[1,2,4,5]School of Engineering, Macquarie University, Sydney, NSW-2109, Australia
[3]School of Electrical and Data Engineering, University of Technology Sydney, NSW-2007, Australia
[*]Corresponding author: vivek.sharma2@hdr.mq.edu.au

***Abstract*—This paper demonstrates the fault tolerance performance of the A-source inverter fed PMSM drive system for electric vehicles. The proposed topology of the A-source impedance network is implemented to obtain high gain dc output for the inverter module. This high magnitude dc output is fed to the PMSM drive system for electric vehicle applications. In addition to the design strategies of the proposed system, this paper presents a fast fault identification and diagnosis strategy under switch faults occurring in the inverter module. The utilized method is robust to common converter issues such as load variations and input power fluctuations. The simulation results of the proposed fault-tolerant operation have been presented in this paper. This efficient fault-tolerant operation substantially improved the reliability of the overall system. The achieved results demonstrate the effectiveness of the proposed system with fault-tolerant capability for electric vehicle applications.**

***Index Terms*—A-source network, fault-tolerant, switch faults, permanent magnet synchronous motor (PMSM) drive, electric vehicles, inverter.**

I. Introduction

The popularity of electric vehicles has gained the attention of researchers across the globe. These vehicles are propelled through electric motors. The most popular choice among those is permanent magnet synchronous motors (PMSM) as they possess several advantages like high efficiency and high-power density [1], [2]. However, for crucial applications, like electric vehicles, involving high speed and variable load operations, these drive systems require higher voltage-boosting control methods. It results in the requirement of larger circuit components which leads to higher cost. In this regard, several converter configurations are proposed. The traditional buck-boost converter topology suffers from drawbacks such as discontinuous input current and charging current, high filter equipment requirement and low efficiency. With the development in configurations, impedance-source converters were proposed [3]. These topologies gained the attraction of the researchers with advantages like high voltage output with single-stage power conversion [4]. Upon integration with the inverter, impedance(Z)-source inverter (ZSI) gained popularity in motor drives applications [5]. In the past decade, many improved configurations of the Z-source networks are proposed with changes in network components arrangements and integrating transformers to obtain high voltage output [6], [7]. However, these configurations are characterized by high voltage stress on the power semiconductor switches, high current ripple and high cost which are not suitable for motor drive applications. In addition to high gain converters, vehicular applications also consist of inverter modules to convert high dc power to ac output for the ac motor drives. It is an inevitable fact that the operation of these motor drives is widely affected by the switch failures in the inverter module that occurred due to open-circuit and short-circuit faults. Any failure in the switch due to open-circuit fault results in the fall of current in the relevant phase and will lead to the shutdown of the system. In addition to it, for a short-circuit fault, the current will be excessively large at the faulted phase. Hence, in order to ensure the reliability of the system for vehicular applications, intelligent control with an efficient fault diagnosis strategy should be developed. Several literature proposed the fault-tolerant remedies for ac motors [8], [9] and permanent magnet synchronous motor (PMSM) drives [10]–[12]. However, these recent fault diagnosis strategies have slow response time and inefficient in preventing the shutdown of the system. The follow-up cost due to faults, service continuity failure, and additional component requirements are a few common concerns to be addressed while designing a fault-tolerant scheme for vehicular applications. It is required to implement reliable fault-tolerant configuration to successfully achieve continuous operation in the event of a fault.

To overcome the above-mentioned issues, an A-source inverter-fed PMSM drive with fault-tolerant capability has been proposed in this paper. This drive is characterized by a high voltage output obtained through a newly developed magnetically coupled impedance source network, called a A-source impedance network. The network provides high voltage gain while operating with a small duty ratio [13], [14]. Subsequently, the proposed system is configured with an efficient fault diagnosis strategy with quick detection and reconfiguration of the circuit to avoid shutdown under the event of a fault. In this paper, the variation in line-to-line voltages and the magnitude of output current are monitored for fault detection. Upon detection of the fault, the gate control is switched to the auxiliary leg. The faulty leg is isolated and the auxiliary leg is connected to the motor terminals to facilitate the continuous power flow. This paper is composed of five sections. Section II describes the design parameters and control schemes of the A-source network-fed PMSM drive system. The proposed fault-tolerant strategy is explained in Section III. The relevant simulation results are presented in Section IV. Finally, a conclusion is presented in Section V.

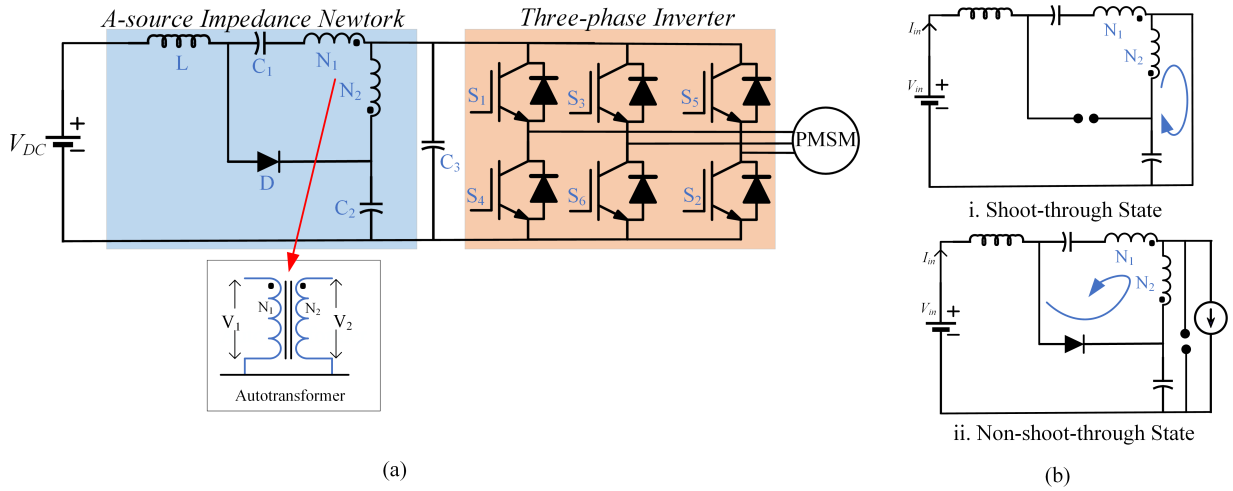

Fig. 1: Proposed System: (a) circuit diagram, (b) operating modes of A-source network.

II. SYSTEM DESCRIPTION

This section aims to describe the design parameters and control schemes for the normal operation of the proposed system. The proposed system is shown in Fig. 1a. It consists of an A-source network to provide high gain dc output from a low voltage input source, a three-phase inverter module to facilitate dc-ac power conversion, and Permanent Magnet Synchronous Motor (PMSM) to drive the electric vehicle.

A. A-source Impedance Network

The low voltage dc input is stepped up to high gain voltage output through the A-source impedance network. It consists of one inductor (L), two capacitors (C_1 and C_2), diode (D), and autotransformer with primary and secondary windings (N_1 and N_2). The high-gain dc output is obtained across dc-link C_3 and acts as input to the inverter module. By utilizing the principle of operation of an autotransformer, high voltage gain can be achieved through a coupled inductor. The voltage gain across autotransformer is given as:

$$\frac{V_2}{V_1} = N \tag{1}$$

where N is called autotransformer turns ratio and is given by

$$N = \frac{N_1 + N_2}{N_1} \tag{2}$$

V_1 and V_2 are the input and output dc voltages respectively. The design specifications for the A-source network are given in [15]. The maximum range of shoot-through duty cycle (D_{st}) for the operation of A-source inverter is given as:

$$0 \leq D_{st} < D_{stmax} = \frac{1}{1+N} \tag{3}$$

The voltage gain is determined as:

$$G = \frac{V_{output}}{V_{input}} = \frac{1}{1-(1+N)D_{st}} \tag{4}$$

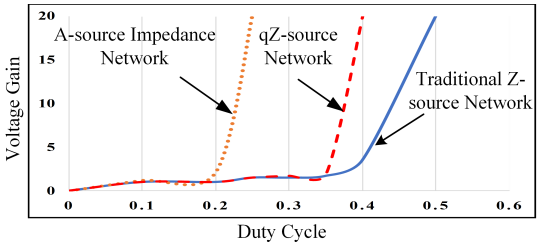

Fig. 2: Voltage gain Comparison.

The A-source impedance network has two modes of operation, as shown in Fig. 1b, which are given as follows:

- Shoot-through State: In this mode, the Diode D is OFF, and the power semiconductor switch is ON. The voltage across inductor L is given as:

$$v_L = V_1 + V_{c2} + \frac{N_2}{N_1}.V_{c1} \tag{5}$$

- Non-shoot-through State: In this state, the diode D is forward biased, and the power semiconductor switch is OFF. The voltage across capacitors is calculated as:

$$v_{c1} = \frac{1-D_{st}}{1-(2+\frac{N_2}{N_1})D_{st}}.V_1 \tag{6}$$

$$v_{c1} = \frac{(\frac{N_2}{N_1}+1)D_{st}}{1-(2+\frac{N_2}{N_1})D_{st}}.V_1 \tag{7}$$

where D_{st} is the shoot-through duty cycle

In addition to it, a comparative analysis of the proposed A-source network with the conventional single-stage power conversion impedance networks is shown in Fig. 2. It can be seen that, in comparison to other high gain impedance networks viz, Z-source and quasi-Z-source networks, the A-source network provides a high boosting capability.

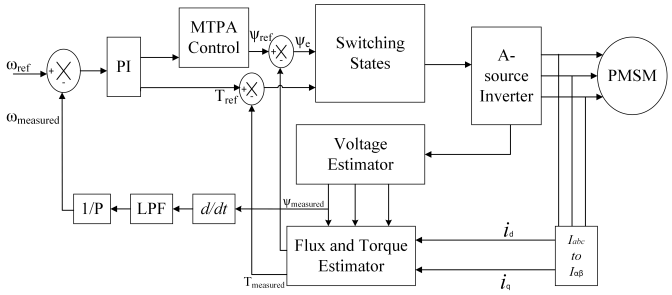

Fig. 3: Control Scheme of PMSM drive system.

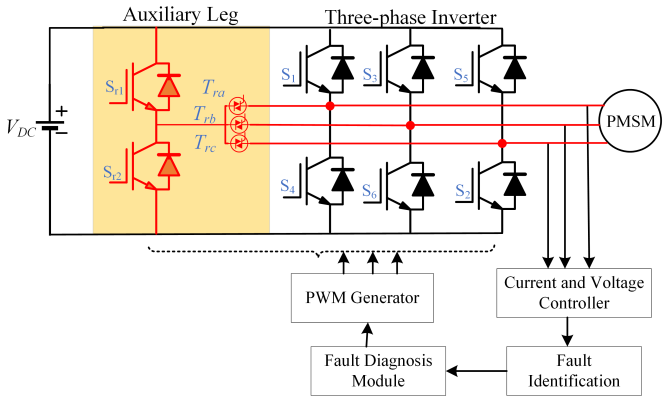

Fig. 4: Fault-tolerant architecture.

B. Permanent Magnet Synchronous Motor (PMSM) Drive

The two level three-phase inverter module facilitates the dc-ac conversion for the PMSM drive. The PMSM is modeled in the rotor reference frame as [16]:

$$\begin{bmatrix} v_{ds} \\ v_{qs} \end{bmatrix} = \begin{bmatrix} R_s + \frac{d}{dt}L_d & -\omega_e L_q \\ \omega_e L_d & R_s + \frac{d}{dt}L_q \end{bmatrix} \begin{bmatrix} i_{ds} \\ i_{qs} \end{bmatrix} + \begin{bmatrix} 0 \\ \omega_e \phi \end{bmatrix} \quad (8)$$

where v_{ds} and v_{qs} are the voltages in d-and q-axis respectively; R_s is the stator resistance, L_d and L_q are the inductances of d-and q-axis respectively; ω_e is the angular frequency; ϕ is the flux linkage; i_{ds} and i_{qs} are the d- and q-axis currents respectively.

The electromagnetic torque is given as:

$$T_e = 3p\frac{\phi I_{qs} + (L_d - L_q) i_{ds} i_{qs}}{2} \quad (9)$$

where p is the number of pole pairs.

The control scheme of the proposed PMSM drive is shown in Fig. 3. The input parameter is the rotor speed and the q-axis current is taken as the output parameter. The estimated rotor speed is estimated through a low-pass filter (LPF) by utilizing the stator flux-linkage vector. The motor controller uses the Park d-q transform which facilitates the elimination of time-varying inductances and provides better control of motor currents and torque. The control operation doesn't provide any field-weakening. The pulse-width modulation (PWM) generation for the inverter switches is based on the switching states. For vehicular applications, the reference torque T_{ref} is obtained by a speed controller based on a proportional-integral (PI) controller. It is implemented to limit the maximum line current of the motor. With variable speed operation, the modulation of the A-source network is adjusted such that the voltage is increased and decreased linearly with the speed. For operations below the rated speed, the dc-link voltage is kept equal to the input voltage. For operations above the rated speed, the dc-link voltage is increased linearly with the speed. In addition to it, the position of the stator flux-linkage vector is determined for every control cycle to implement the fault-tolerant control scheme. In order to calculate the reference flux, maximum torque per ampere (MTPA) control is used [17]. The maximum-torque-per-ampere (MTPA) control strategy is the best approach to obtain high efficiency for operations below the rated speed. The torque and current utilization will be maximum through this control strategy. It minimizes the copper loss.

III. Fault-tolerant Strategy

Fault-tolerant operation is much appreciated in applications like automotive industries, which requires high-reliability operations. An effective fault-tolerant operation facilitates the post-fault operation similar to the normal operation of the motor drive. The fault-tolerant architecture for the proposed system is shown in Fig. 4. In this paper, the fault-tolerant operation involves the implementation of the additional leg, called the auxiliary leg, in addition to the three-phase legs of the inverter module. The additional leg will be connected to the overall system in the event of a fault. An improved control strategy is proposed to detect and localize the fault. It is a well-known fact that the power semiconductor switches are highly prone to failures due to open- and short-circuit faults during long-hour operations. Hence, it will be an effective way to improve the reliability of the proposed motor drive system by considering such faults to design fault-tolerant strategies.

In this paper, the simulation studies are performed for the following case studies of different faults that can affect the drive's operation:

1) open-circuit fault in single-IGBT
2) open-circuit fault in phase-leg
3) short-circuit fault in single-IGBT
4) short-circuit fault in phase-leg

The fault-tolerant operation involves; (i) fault identification, and (ii) Isolation and remedial measures. The fault identification method determines the nature of the fault. Upon detection, the modulation signal of the faulted phase is switched to the auxiliary leg in order to maintain service continuity.

A. Fault Identification

In order to identify open-circuit fault, the fault detection is performed by measuring the line-to-line voltage deviations. The line-to-line voltages under normal operation are given by

$$\begin{bmatrix} V_{ab} \\ V_{bc} \\ V_{ca} \end{bmatrix} = \begin{bmatrix} 1 & -1 & 0 \\ 0 & 1 & -1 \\ -1 & 0 & 1 \end{bmatrix} \begin{bmatrix} V_{an} \\ V_{bn} \\ V_{cn} \end{bmatrix} \quad (10)$$

where V_{an}, V_{bn}, V_{cn} are the phase voltages.

During the event of open-circuit fault in IGBT of phase-A, the line-to-line voltage is given as:

$$\begin{bmatrix} V_{abF} \\ V_{bcF} \\ V_{caF} \end{bmatrix} = \begin{bmatrix} 1 & -1 & 0 \\ 0 & 1 & -1 \\ -1 & 0 & 1 \end{bmatrix} \begin{bmatrix} V_{an} \\ V_{bn} \\ V_{cn} \end{bmatrix} + \begin{bmatrix} -\Delta V_{an} \\ \Delta V_{bn} \\ \Delta V_{cn} \end{bmatrix} \quad (11)$$

where V_{abF}, V_{bcF}, V_{caF} denotes line-to-line voltages during fault.

The voltage deviations under open-circuit fault are given as:

$$\Delta V_{xy} = V_{xy} - V_{xyF} \quad (xy \in ab, bc, ca) \quad (12)$$

Upon identification of the finite value of voltage deviation, the fault status is confirmed by generating an error signal.

On the contrary, if the gate signal to the switch is identified as low while the current across the switch is high, the condition is identified as a short-circuit fault. The proposed fault diagnosis logic for identifying the short-circuit fault is based on the concept that when the gate signal is low, the current should be zero. Hence, a short-circuit fault is asserted if the switch current is non-zero for a low gate signal. To operate the drive at high-current, fast-acting fuses can be added to the existing architecture for better protection of the circuit components.

B. Isolation and Remedial Measures

After the fault is detected, the faulty leg or switch is isolated by using the TRIAC arrangement (T_{ra}, T_{rb}, T_{rc}). The TRIACs are used to connect the auxiliary leg to the phase legs of the three-phase inverter module. The isolation of a faulty leg is implemented by disabling the gating signals to the faulted phase and the gating signals are routed to activate the auxiliary leg connection. The normal operation of the system is resumed. Therefore, the shutdown of the system under a faulty condition can be prevented by utilizing the proposed fault-tolerant scheme. As this changeover doesn't change the topology of the system, the modulation schemes and control algorithms remain unchanged. Hence, the cost of the circuit and the time required for the reconfiguration of the circuit is very low. Therefore, fault diagnosis is very quick. The fault diagnosis is achieved in less than one switching cycle. In addition to it, the unbalancing across capacitor voltages are prevented by auxiliary leg configuration. This results in lower voltage stress across the switches. The positive and negative values of the output voltage of the faulty phase can be generated using the proposed fault-tolerant control. Hence the proposed system can operate at a high modulation index. This feature allows for obtaining high voltage gain through the A-source impedance network.

It should be noted that the proposed fault-tolerant configuration can handle all the possible switch failures under open-circuit and short-circuit faults; provided all the switches doesn't fail simultaneously. Under the event of faults, the proposed fault-tolerant topology enables the motor-drive system to maintain a efficient post fault operation without compromising the power output. This advantage makes the system suitable for electric vehicle application.

TABLE I: Circuit Parameters

Parameter	*Symbol*	*Value*
A-source network		
Input Voltage	V_{in}	100 V
Output Voltage	V_o	220 V
Capacitance	C_1 C_2	220 μ F 100 μ F
Inductor	L	330 mH
Turns ratio	$N_1 : N_2$	1:2
PMSM Drive		
Nominal Speed	N_r	3000 rpm
Nominal Current	I_{rated}	6.1 A
Maximum Rated DC bus Voltage	V_{DC}	300 V
Maximum Torque	T_{max}	1.65 N-m
Nominal Torque	T_{rated}	0.41 N-m
Nominal Power	P_{out}	1.5 kW
Stator resistance	R_s	0.02 Ω
Inertia	J	100 kg-m^2
Magnetic flux	ϕ_r	0.35 Wb
Number of pole pairs	p	3
q-axis inductance	L_d	27 mH
d-axis inductance	L_d	9.94 mH

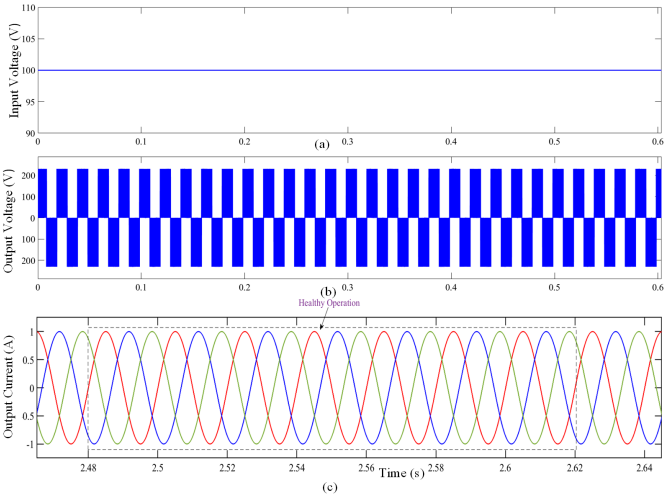

Fig. 5: Simulation waveforms under normal operation: (a) input voltage, (b) output voltage, and (c) output current.

IV. Simulation Results

The simulation experiments for the proposed A-source fed PMSM drive system is carried out to investigate the system performance. The system parameters are listed in Table I. It is worth highlighting that the achieved voltage gain is 2 for the proposed system. It facilitates the high output voltage output of 220V from an input supply of 100V.

A. Normal Operation

The input voltage, output voltage and output current waveforms under normal operation are shown in Fig. 5. The proposed converter-inverter arrangement provides ripple-free output to the motor drive system.

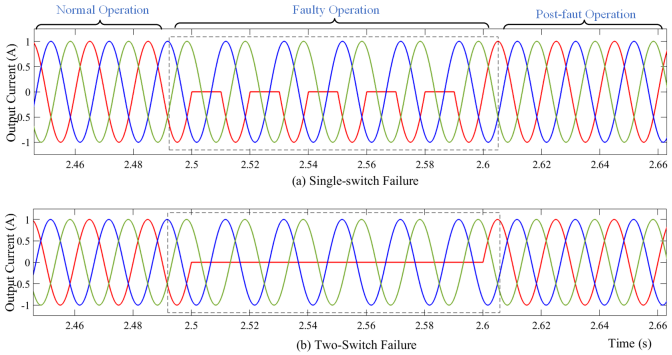

Fig. 6: Simulation waveforms under fault-tolerant operation.

B. Fault-tolerant Operation

In this paper, the faults are introduced in the switches of phase-A of the inverter module. Due to the catastrophic effects of short-circuit faults in the system, these faults are turned into open-circuit faults using the fault isolating circuits. The proposed fault-tolerant strategy is carried out after successful fault detection. Upon detection, the identification algorithm is followed to determine the exact fault location. The output current under the fault-tolerant operation is shown in Fig. 6. It can be observed that due to single-switch failure only one-half of the output waveform is obtained whereas for the two-switch failure of the same leg, the output current in the respective phase is zero. The fault is detected, and the reconfiguration configuration of the system is applied. It can be also be seen in Fig. 6 that due to the proposed fault diagnosis scheme; the motor current is brought back to the rated value. The service continuity is maintained during the post-fault operation. The proposed reconfiguration can effectively avoid the overcurrent and overvoltage phenomenon. It takes less than one switching cycle for the diagnosis strategy to track the measured value of the current. This study is carried out at a high switching frequency of 10kHz. In the case of lower switching frequency operation, the fault detection time could be longer. In that case, high current-rating fuses must be added to the given system for the protection of the circuit. Due to symmetry of configuration, the same fault-tolerant configuration can be applied for switch failures occurring in the other two phases *(phase-B and phase-C)*.

C. Performance Evaluation for Electric Vehicles

For vehicular applications, the proposed system is subjected to the New European Driving Cycle (NEDC) to test its electric energy consumption. All-electric vehicles should comply with the legislative New European Driving Cycle (NEDC) specified in current emissions legislation. It is performed to prove the suitability of the vehicle for real-world driving data. The driving cycle response of the proposed motor-drive system is shown in Fig. 7a. It can be observed in Fig. 7a that the motor precisely follows the reference NEDC driving cycle under the fault-tolerant operation.

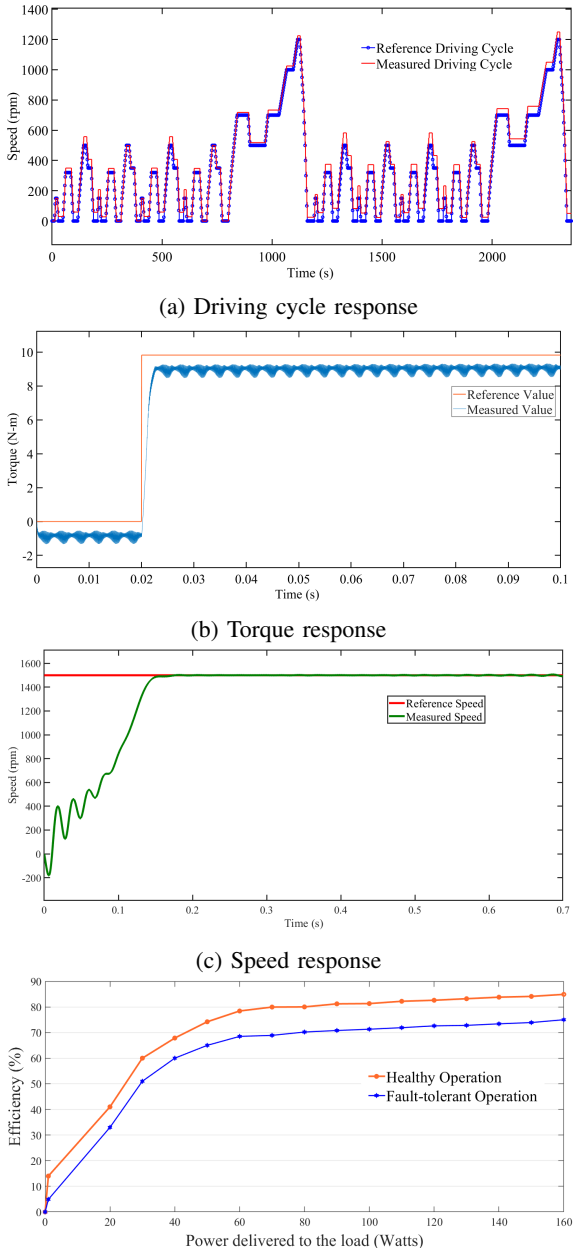

(a) Driving cycle response

(b) Torque response

(c) Speed response

(d) Efficiency Curve

Fig. 7: System responses for electric vehicle application.

Also, the torque and speed response of the proposed motor system are presented during the fault-tolerant operation in Fig. 7b and Fig. 7c. It is observed in Fig. 7b that the available torque decreases due to the fault. However, with the proposed fault-tolerant strategy the motor torque is compensated back to the rated value and have better behavior in response to the load variations. In addition to it, it can be seen in Fig. 7c that the speed curve follows the reference speed during the fault-tolerant operation. It can be clearly inferred that with the proposed strategy, the measured speed more accurately tracks the reference rated speed. The electric vehicles require large torque during starting, during climbing a slope, and during ac-

celeration. Subsequently, the constant output power is required during high-speed operations of the vehicle. The speed-torque characteristics of the proposed motor drive system can satisfy the demand of electric vehicles requiring large torque at low speed and constant power at high speed.

In addition to it, the motor efficiency curve is plotted for the fault-tolerant operation. It can be seen in Fig. 7d that the motor efficiency is not degraded to a larger value due to the fault-tolerant capability. The proposed system achieved an efficiency of nearly 85 % of the normal operation. The achieved results show that the proposed system is compatible for electric vehicle applications.

V. Conclusion

This paper has discussed the fault tolerance performance of the A-source inverter fed PMSM drive system. The proposed system is characterized by high voltage output and a fast fault-diagnosis strategy. This study provides an efficient solution for switch failures commonly occurring due to open- and short-circuit faults in the inverter module. It demonstrates a fault-tolerant operation which enables the overall system to be operational after the fault. The compensation strategy facilitates service continuity in the event of faults. This method is robust for asymmetrical conditions that might occur due to load variations and input disturbances. The proposed method is advantageous in terms of fast detection time and the better torque-speed response of the motor drive system during fault-tolerant operation. The proposed system is compatible for crucial applications of PMSM drive such as electric vehicles.

The proposed system can be extended for other dc-dc converters such as buck-boost, cuk, and several other topologies of impedance source networks. In the future, the validation of the theoretical analysis will be performed on the experimental setup.

References

[1] X. Sun, Z. Shi, G. Lei, Y. Guo and J. Zhu, "Analysis and Design Optimization of a Permanent Magnet Synchronous Motor for a Campus Patrol Electric Vehicle," in IEEE Trans. on Vehicular Technology, vol. 68, no. 11, pp. 10535-10544, Nov. 2019.

[2] Y. Dai, L. Song and S. Cui, "Development of PMSM Drives for Hybrid Electric Car Applications," IEEE Trans. on Magnetics, vol. 43, no. 1, pp. 434-437, Jan. 2007.

[3] Fang Zheng Peng, "Z-source inverter," IEEE Trans. on Ind. Appl., vol. 39, no. 2, pp. 504-510, March-April 2003.

[4] V. Sharma, P. Saini, S. Garg and B. Negi, "Comparative analysis of VSI, CSI and ZSI fed induction motor drive system," 2016 3rd International Conference on Computing for Sustainable Global Development (INDIACom), New Delhi, 2016, pp. 1188-1191.

[5] Fang Zheng Peng et al., "Z-source inverter for motor drives," in IEEE Trans. on Power Electron., vol. 20, no. 4, pp. 857-863, July 2005.

[6] Y. P. Siwakoti, F. Z. Peng, F. Blaabjerg, P. C. Loh and G. E. Town, "Impedance-Source Networks for Electric Power Conversion Part I: A Topological Review," IEEE Tran. on Power Electron., vol. 30, no. 2, pp. 699-716, Feb. 2015.

[7] P. C. Loh and F. Blaabjerg, "Magnetically Coupled Impedance-Source Inverters," IEEE Trans. on Ind. Appl., vol. 49, no. 5, pp. 2177-2187, Sept.-Oct. 2013.

[8] V. Sharma, M. J. Hossain, S. M. N. Ali and M. Kashif, "Bi-directional TRIAC fault-protection technique for Z-source half-bridge converter-fed AC motor Drives," 2018 Australasian Universities Power Engineering Conference (AUPEC), Auckland, New Zealand, 2018, pp. 1-6.

[9] V. Sharma, M. J. Hossain and S. M. N. Ali, "Fault Protection Technique for ZSI-fed Single-Phase Induction Motor Drive System," 2018 IEEE Region Ten Symposium (Tensymp), Sydney, Australia, 2018, pp. 30-35.

[10] X. Zhou, J. Sun, H. Li and X. Song, "High Performance Three-Phase PMSM Open-Phase Fault-Tolerant Method Based on Reference Frame Transformation," in IEEE Trans. on Ind. Electron., vol. 66, no. 10, pp. 7571-7580, Oct. 2019.

[11] S. K. Kommuri, M. Defoort, H. R. Karimi and K. C. Veluvolu, "A Robust Observer-Based Sensor Fault-Tolerant Control for PMSM in Electric Vehicles," in IEEE Trans. on Ind. Electron., vol. 63, no. 12, pp. 7671-7681, Dec. 2016.

[12] R. R. Errabelli and P. Mutschler, "Fault-Tolerant Voltage Source Inverter for Permanent Magnet Drives," in IEEE Trans. on Power Electron., vol. 27, no. 2, pp. 500-508, Feb. 2012.

[13] S. Esmaeili, S. Karimi, A. Mostaan, A. Iqbal and A. Siadatan, "A Family of High Step-Up A-Source Inverters with Clamped DC-Link Voltage," 2019 10th International Power Electronics, Drive Systems and Technologies Conference (PEDSTC), Shiraz, Iran, 2019, pp. 195-200.

[14] A. Ayachit, Y. P. Siwakoti, V. P. N. Galigekere, M. K. Kazimierczuk and F. Blaabjerg, "Steady-State and Small-Signal Analysis of A-Source Converter," in IEEE Trans. on Power Electron., vol. 33, no. 8, pp. 7118-7131, Aug. 2018.

[15] Y. P. Siwakoti, F. Blaabjerg, V. P. Galigekere, A. Ayachit and M. K. Kazimierczuk, "A-Source Impedance Network," in IEEE Trans. on Power Electron., vol. 31, no. 12, pp. 8081-8087, Dec. 2016.

[16] P. Liu and H. P. Liu, "Permanent-magnet synchronous motor drive system for electric vehicles using bidirectional z-source inverter," in IET Electrical Systems in Transportation, vol. 2, no. 4, pp. 178-185, December 2012.

[17] M. Khayamy and H. Chaoui, "Current Sensorless MTPA Operation of Interior PMSM Drives for Vehicular Applications," IEEE Trans. on Vehicular Technology, vol. 67, no. 8, pp. 6872-6881, Aug. 2018.